Manuscript_BEES_Bima Gilang Pratama.pdf

by Tugiminoye01@gmail.com 1

Submission date: 03-Jul-2025 11:08PM (UTC-0400)
Submission ID: 2643469999
File name: Manuscript_BEES_Bima_Gilang_Pratama.pdf (650.75K)
Word count: 5456
Character count: 30288

Website https://ejournal.seminar-id.com/index.php/bees

BEES: Bulletin of Electrical and Electronics Engineering

ISSN 9999-9999 (Media Online), Vol x, No x, Month Year, pp 999-999
DOI 10.47065/bees.v9i9.9999

Voltage Flicker Analysis due to the Starting of a 250 kW Three-Phase Induction Motor at the SWK Karah Pump House, Surabaya

Reza Sarwo Widagdo[1*], Pujislamet[2], Indra Budi Hermawan[3], Bima Gilang Pratama[4]
[1,2,3,4]Department of Electrical Engineering, Universitas 17 Agustus 1945 Surabaya, Indonesia
Email: [1*]rezaswidagdo@untag-sby.ac.id, [2]pujislamet@untag-sby.ac.id, [3]indra@untag-sby.ac.id,
[4]bimagilangpratama19@gmail.com

ARTICLE INFORMATION

Article History:
Submited : 00 Bulan 0000
Accept : 00 Bulan 0000
Published : 00 Bulan 0000

CORESSPONDENCE
Email: rezaswidagdo@untag-sby.ac.id

A B S T R A C T

This study aims to identify the main factors contributing to voltage flicker during the starting process of a 250 kW three-phase induction motor at the SWK Karah Pump House in Surabaya. The use of high-power induction motors in pump houses is critical for supporting flood control efforts in Surabaya. However, conventional starting methods such as Direct On Line (DOL) and Star-Delta can produce high inrush currents, potentially causing significant voltage flicker. This research analyzes the magnitude of the starting current, calculates the total impedance of the distribution system, and evaluates the resulting voltage flicker during motor startup. The methodology includes calculations of cable and transformer impedance, along with analysis of starting current and voltage in accordance with IEC 61000-4-15 standards. The results indicate that the DOL method produces a starting current of 1.710,61 A (approximately 2,88 times the nominal current), leading to substantial RMS voltage drop and voltage flicker of 32,48%. In contrast, the Star-Delta method reduces the starting current to 570,20 A (approximately 0,96 times the nominal current), resulting in much lower voltage flicker of around 11%, although careful consideration of the transition duration is still required. The analysis concludes that direct starting of large induction motors without adequate current control can significantly degrade power quality and disrupt the stability of the pump house distribution system. Both methods, despite Star-Delta's improvement, still have the potential to exceed the short-term severity limits for voltage flicker specified in IEC 61000-4-15 if the distribution system lacks sufficient mitigation equipment..

Keywords: 3 Phase Induction Motor, Direct On-Line (DOL), Flicker, Star Delta

1. INTRODUCTION

Urban areas around the world increasingly face significant challenges in managing water resources, particularly in controlling flooding exacerbated by high rainfall during wet seasons. Rising precipitation patterns, often influenced by climate variability, directly increase the risk of urban flooding. To address this issue, flood pump stations serve as essential components of urban drainage systems, designed to rapidly channel stormwater away from residential and commercial areas to reduce inundation and control flood levels. These pump stations are typically equipped with large-capacity pumps driven by three-phase induction motors, which are widely used for their reliability and robustness in heavy-duty applications. However, these high-power motors require substantial electrical energy to operate. A critical consideration is the very high inrush (starting) current that occurs when these motors are energized. Starting currents can reach 6 to 10 times the motor's rated current, potentially causing significant disturbances in the electrical distribution system in the form of momentary voltage drops. Such disturbances, commonly referred to as voltage flicker, are characterized by rapid variations in RMS voltage that can lead to perceptible lamp flickering and may interfere with sensitive electronic equipment such as programmable logic controllers (PLCs) and other control devices. The operational reliability of flood pump stations and indeed many forms of critical infrastructure depends heavily on the stability and quality of their electrical power supply [1],[2].

Power quality disturbances such as voltage flicker not only risk damaging electrical equipment but can also impair the ability of pumps to operate effectively during critical flood events. This, in turn, can compromise the effectiveness of flood mitigation efforts and pose risks to public safety and urban resilience. Therefore, a thorough analysis of the impact of starting large three-phase induction motors on voltage flicker is essential for planning, designing, and operating reliable flood-control infrastructure. A comprehensive understanding of this phenomenon can support the development of effective strategies to mitigate flicker, ensuring stable and high-quality power supply. More broadly, power quality has become a central concern in modern industrial systems and critical infrastructure. The growing use of sensitive electronic devices and the demand for continuous, reliable operation necessitate a stable, high-quality power supply [3]. Large inductive loads, such as high-power induction motors, are recognized as significant contributors to power quality issues, particularly during transient starting phases. International standards such as IEC 61000-4-15 provide a framework for assessing and managing voltage flicker, helping ensure acceptable power quality levels in electrical distribution systems [4].

Previous studies have extensively examined voltage flicker caused by induction motor starting. Tampubolon and Yana [5] investigated general voltage flicker caused by induction motor starting and its impact on sensitive electronic devices. While providing a foundational understanding, their study did not specifically focus on critical infrastructure contexts or quantitative comparisons of starting methods for high-power motors. Permana *et al.* [6] conducted simulation-based analysis using ETAP 12.6 for various starting methods (Direct On Line (DOL), Soft Starting, and Variable Frequency Drive (VFD)) in power plants, concluding that VFD is the most effective method for mitigating flicker. Their work offers valuable benchmarks for advanced methods and simulation-based analysis but differs from this study's empirical measurement approach for traditional starting methods on a specific high-power motor. Altaira et al. [7] generally discussed voltage sags caused by starting large-capacity motors and highlighted the importance of applying appropriate starting methods to reduce high inrush currents. Although acknowledging the issue, that study did not provide detailed comparative quantitative analysis of the most common starting methods for motors with capacities and applications like those examined here. Nema & Tomar [8] compared autotransformer, reactor, and star-delta methods for much larger motors (2500 kW), offering insights into mitigation techniques for very high-power applications. However, the present study focuses on a more typical industrial motor size with direct empirical comparison between DOL and Star-Delta, filling a gap for this specific power range and application.

Negi et al. [9] performed a comparative analysis of DOL, Star-Delta, and Autotransformer methods, showing flicker percentages and current ratios for much smaller motors. However, power quality issues scale strongly with motor size and system impedance. This study provides essential empirical data for much larger motors, where the impact on the electrical grid is far more significant, thus addressing important gaps in the literature on high-power motor starting in critical infrastructure. Although existing literature has extensively discussed voltage flicker phenomena and various motor starting methods, there remains a specific research gap in empirical, measurement-based comparative analyses of Direct on Line (DOL) and Star-Delta methods applied to three-phase induction motors operating in critical flood-control pump houses. Prior studies often rely on simulations, focus on smaller motor sizes, or address different industrial contexts, limiting their direct applicability to large-scale urban drainage infrastructure. The novelty of this research lies in its focus on real-world measurement and analysis of starting currents and voltage flicker in an actual urban pump station environment using a high-power induction motor. By providing detailed empirical data under realistic operating conditions, this study delivers practical and actionable insights for engineers and utility planners seeking to improve power quality and ensure the reliable operation of vital urban infrastructure. The primary objective of this research is to analyze the causes of voltage flicker during the starting of a 250 kW three-phase induction motor at a flood-control pump house. Furthermore, this study aims to evaluate how the starting method affects voltage flicker in the electrical system and to quantify its impact on power quality, particularly in terms of voltage flicker severity. Ultimately, the research seeks to identify effective mitigation strategies to ensure reliable and stable pump operation during critical flood events.

2. RESEARCH METHOD

This study was conducted at the SWK Karah Flood Pump Station in Surabaya during March 2025, focusing on the starting behavior of a 250 kW three-phase induction motor. The research involved field measurements of starting current and voltage flicker using a Fluke 305 clamp meter, selected for its ability to safely measure electrical parameters in live systems. Motor specifications were obtained from the nameplate and used in conjunction with system impedance data to perform analytical calculations. Field observations and interviews with operational personnel complemented the quantitative data, ensuring a comprehensive understanding of the motor's impact on power quality during startup.

2.1 Total Impedance Analysis of the Distribution Network

In analyzing the power distribution system, determining the total impedance from the transformer to the motor load is essential, as it directly influences voltage drop and overall system performance. This analysis considers the system base impedance, transformer impedance, and cable impedance. Determining the total impedance from the transformer to the motor is crucial for analyzing voltage drop and system performance. The base impedance is calculated using:

$$Z_{Base} = \frac{V_S^2}{S} \quad (1)$$

Transformer impedance is obtained from its percentage rating:

$$Z_{Trafo} = \frac{\%Z}{100} \times Z_{Base} \quad (2)$$

Cable impedance depends on length and per-kilometer values:

$$Z_{Cables} = length \times (R' + jX') \quad (3)$$

The total network impedance sums transformer and cable values:

$$Z_{total} = Z_{Trafo} + Z_{Cables} \quad (4)$$

This total impedance is a key parameter for evaluating voltage drop during motor starting. The base impedance is calculated from the system's nominal voltage and transformer capacity and serves as a reference for per-unit calculations. Transformer impedance, typically given as a percentage, is converted to ohms for detailed analysis, while cable impedance depends on conductor length and specified impedance per kilometer. The total network impedance is obtained by summing transformer and cable impedances, representing the overall resistance and reactance between the power source and motor load.

2.2 Thevenin Impedance Calculation for the 250 kW Motor

The Thevenin impedance of the three-phase 250 kW induction motor represents the effective impedance seen from the supply side to the motor terminals. This impedance combines the stator and rotor resistances and reactances into a single complex value. It is a critical parameter for modeling motor starting behavior, as it determines how much voltage drop occurs during high inrush currents and directly affects voltage flicker during motor startup. The motor's Thevenin impedance combines stator and rotor resistance and reactance [10]:

$$Z_{th\,(motor)} = (R_S + R_r) + j(X_s + X_r) \quad (5)$$

Its magnitude is computed by:

$$|Z_{th}| = \sqrt{(Rs + R_r)^2 + (Xs + X_r)^2} \quad (6)$$

This parameter represents the effective source impedance seen by the motor during starting.

2.3 Starting Current Analysis with Direct On Line (DOL) Method

The Direct On Line starting method is a simple and common approach where the motor is connected directly to the full supply voltage. This results in very high starting current, typically several times the motor's rated current. Calculating the starting current using the Thevenin impedance helps estimate the magnitude of inrush current and predict its potential to cause severe voltage flicker. This analysis highlights why DOL starting can lead to substantial voltage disturbances in the power system, especially with large motors. DOL starting connects the motor directly to full voltage, resulting in high inrush current [11]:

$$I_{(start)DOL} = \frac{V}{Z_{th\,(motor)}} \quad (7)$$

The ratio to rated current is evaluated by:

$$I_{(start)DOL} = n \times I_{rated} \quad (8)$$

This large inrush current can cause severe voltage flicker.

2.4. Starting Current Analysis with Star-Delta Method

The Star-Delta starting method aims to reduce inrush current by initially connecting the motor windings in a star configuration before switching to delta. This approach lowers the starting current to approximately one-third of the DOL value. The reduced inrush current significantly decreases the risk of voltage flicker and mitigates adverse impacts on power quality, making it a widely used method for large motors in critical applications. Star-Delta starting reduces inrush current by initially connecting in star, then switching to delta [12]:

$$I_{(start)Y-\Delta} = \frac{1}{3} \times I_{(start)DOL} \tag{9}$$

Its ratio to rated current is:

$$I_{(start)Y-\Delta} = n \times I_{rated} \tag{10}$$

This method significantly mitigates voltage flicker compared to DOL.

2.4. Voltage Flicker Estimation for DOL Starting

Voltage flicker results from the significant voltage drop caused by large inrush currents during motor starting. For the DOL method, the expected voltage drop is estimated by multiplying the high starting current by the total network impedance. The percentage voltage flicker is then calculated relative to the system's nominal voltage. This analysis demonstrates the severe voltage fluctuations that can occur with DOL starting, potentially exceeding acceptable limits and disrupting other connected loads. Voltage drop during DOL starting is estimated by [13]:

$$V_{drop(DOL)} = Z_{total} \times I_{start(DOL)} \tag{11}$$

Percentage flicker is calculated as:

$$\%Flicker = \frac{V_{drop\,(DOL)}}{V_{rated}} \times 100\% \tag{12}$$

This highlights the substantial flicker risk of DOL starting.

2.5 Voltage Flicker Estimation for Star-Delta Starting

For the Star-Delta method, the lower starting current leads to a much smaller voltage drop across the distribution network impedance. Estimating the resulting voltage flicker percentage shows the improvement achieved with this method. Although significantly reduced compared to DOL, the residual flicker still requires consideration to ensure compliance with power quality standards, especially in systems serving sensitive equipment. For Star-Delta starting, the voltage drop is [14]:

$$V_{drop(Y-\Delta)} = Z_{total} \times I_{start(Y-\Delta)} \tag{11}$$

Percentage flicker is computed as:

$$\%Flicker = \frac{V_{drop(Y-\Delta)}}{V_{rated}} \times 100\% \tag{12}$$

This shows the reduced flicker achieved with Star-Delta starting, supporting its use in power-quality-sensitive systems.

2.7 3-Phase Induction Motor Specification

The focus of this study is a 250 kW three-phase induction motor installed at the pump station. Nameplate specifications and equivalent circuit parameters were recorded to support calculations and analysis of starting currents and voltage flicker levels.

Table 1. Motor Specification

Description	Parameter
Motor Power (P)	250 kW
Voltage (V_{rated})	400 V
Current (I_{rated})	450 A
Frequency (f)	50 Hz
Efficiency	0,82
Power Factor (Cos φ)	0,9
Synchronous Speed	1500 rpm (4 pole)

Based on Table 1, this induction motor has a power rating of 250 kW, operates at 400 V, and has a rated current of 450 A. It is designed for 50 Hz frequency, with an efficiency of 0.82 and a power factor of 0.9. The motor's synchronous speed is 1500 rpm, indicating that it has 4 poles. In addition to these general specifications, the equivalent circuit parameters of the induction motor are also crucial for performance analysis, particularly for calculating starting current and voltage flicker. These parameters represent the internal resistance and reactance characteristics of the motor. Table 2 shows the equivalent circuit parameters of the 250 kW 3-phase induction motor.

Table 2. Equivalent Parameter

Description	Value
Stator Resistance (R_S)	0,03 Ω
Rotor Resistance (R_r)	0,02 Ω
Stator Reactance (X_S)	0,12 Ω
Rotor Reactance (X_r)	0,12 Ω

These parameters stator resistance (Rs), rotor resistance (Rr), stator reactance (Xs), and rotor reactance (Xr) are used to construct the motor's equivalent circuit model. This model enables accurate theoretical calculations of the motor's behavior during starting, including the magnitude of inrush current and the total impedance seen from the source side, which is a key factor in determining the level of voltage flicker.

3. RESULT AND DISCUSSION

This section presents the results of the calculations and analyses related to the electrical performance of the distribution network and induction motor during starting conditions. The calculations cover total network impedance, the Thevenin equivalent impedance of the motor, starting currents using Direct On Line (DOL) and Star-Delta methods, and the resulting voltage flicker. Each subsection begins with an introduction describing the objective and context, followed by detailed calculation steps and a discussion of the results. This structured approach supports a clear understanding of the impact of large motor starting on power quality and system stability.

3.1 Analysis of Total Impedance Calculation in the Distribution Network

In power distribution system analysis, determining the total impedance along the path from the transformer to the motor load is a critical step. This impedance directly influences voltage drops, short-circuit currents, and overall system performance. By calculating the combined impedance of the transformer and the connecting cables, engineers can predict how the system will respond to high starting currents, evaluate voltage stability, and design mitigation strategies to maintain power quality. The base impedance is calculated using:

$$Z_{Base} = \frac{V_s^2}{S} = \frac{400^2}{200.000} = 0{,}8\ \Omega$$

The transformer impedance is:

$$Z_{Trafo} = \frac{\%Z}{100} \times Z_{Base} = \frac{6}{100} \times 0{,}8 = 0{,}048\ \Omega$$

The cable impedance over 200 m (0.2 km) with known $Z' = 0{,}15 + j0{,}08\ \Omega$/km

$$Z_{Cables} = l \times (R' + jX') = 0{,}2 \times (0{,}15 + j0{,}08) = 0{,}03 + j0{,}016\ \ \Omega$$

Magnitude:

$$|Z_{Cable}| = \sqrt{(0{,}03^2 + 0{,}016^2)} = 0{,}0337\ \Omega$$

Total network impedance:

$$Z_{total} = Z_{Trafo} + Z_{Cables} = 0{,}048 + 0{,}0337 = 0{,}0817\ \Omega$$

The total impedance of 0,0817 Ω reflects the combined resistance and reactance between the transformer and the motor load. This value is crucial for assessing expected voltage drops during motor starting, which can affect power quality and operational reliability in the distribution system.

3.2 Analysis of Thevenin Impedance of the Three-Phase Induction Motor

This subsection focuses on determining the Thevenin equivalent impedance of the 250 kW three-phase induction motor, as viewed from the power source. The Thevenin impedance is essential for modeling the motor's internal characteristics during starting. It enables engineers to predict inrush current levels and analyze the motor's interaction with the distribution system, supporting strategies to mitigate voltage dips and protect system stability.

$$Z_{th} = (R_S + R_r) + j(X_s + X_r) = (0{,}03 + 0{,}02) + j(0{,}12 + 0{,}12) = 0{,}05 + j0{,}24$$

Magnitude:

$$|Z_{th}| = \sqrt{(Rs + R_r)^2 + (Xs + X_r)^2} = \sqrt{(0{,}05)^2 + (0{,}24)^2} = 0{,}245\ \Omega$$

The calculated Thevenin impedance of 0.245 Ω represents the motor's effective internal opposition to current flow during starting. This parameter is vital for estimating inrush currents that can cause voltage flicker and stress on the electrical network.

3.3 Analysis of Starting Current Using Direct On Line (DOL) Method

This subsection analyzes the starting current of the 250 kW three-phase induction motor when using the Direct On Line (DOL) starting method. In DOL starting, the motor is connected directly to the full supply voltage, resulting in a high inrush current. Understanding the magnitude of this starting current is essential for assessing its impact on voltage stability and the potential for power quality disturbances in the network.

$$I_{(start)DOL} = \frac{V}{Z_{th}} = \frac{419{,}2}{0{,}245} = 1.710{,}61\ \text{A}$$

Comparison with rated current ($I_{rated} = 592{,}70$ A) :

$$n = \frac{I_{(start)DOL}}{I_{rated}} = \frac{1.710{,}61}{592{,}70} = 2{,}88\ \text{times}$$

The calculation shows that the DOL starting method results in a starting current approximately 2,88 times the rated current. This large inrush current can cause significant voltage dips, stress motor windings, and negatively affect other connected equipment.

3.4 Analysis of Starting Current Using Star-Delta Method

This subsection evaluates the starting current when the motor uses the Star-Delta starting method. The Star-Delta technique initially connects the motor in a star configuration to reduce the applied voltage and starting current before switching to delta for normal operation. Calculating the reduced starting current helps demonstrate the method's effectiveness in minimizing voltage disturbance and mechanical stress.

$$I_{(start)Y-\Delta} = \frac{1}{3} \times I_{(start)DOL} = \frac{1}{3} \times 1{,}710{,}61 = 570{,}20\ \text{A}$$

Comparison with rated current:

$$n = \frac{I_{(start)\,Y-\Delta}}{I_{rated}} = \frac{570{,}20}{592{,}70} = 0{,}96\ \text{times}$$

The Star-Delta starting method reduces the inrush current to about 96% of the motor's rated current. This significant reduction helps improve voltage stability and limits the impact of motor starting on other loads connected to the same network.

3.5 Calculation of Voltage Flicker Caused by DOL Starting

This subsection calculates the voltage drop, or flicker, resulting from the large starting current when using the DOL method. Voltage flicker is a visible effect of voltage dips that can affect customer equipment. Quantifying this impact is essential for evaluating whether the DOL starting method meets acceptable power quality standards.

$$V_{drop(DOL)} = Z_{total} \times I_{start(DOL)} = 0{,}0796 \times 1.710{,}61 = 136{,}16\ \text{V}$$

Percentage flicker:

$$\%Flicker = \frac{V_{drop\ (DOL)}}{V_{rated}} \times 100\% = \frac{136{,}16}{419{,}10} \times 100\% = 32{,}48\%$$

The result shows a flicker level of 32.48%, indicating a severe voltage dip during DOL starting. Such a high level of voltage disturbance is likely unacceptable in most power systems, underscoring the need for alternative starting methods or mitigation strategies.

3.6 Calculation of Voltage Flicker Caused by Star-Delta Starting

This subsection examines the voltage flicker caused by starting the motor with the Star-Delta method. By reducing starting current, the Star-Delta method aims to minimize the resulting voltage dip, making it an attractive option for improving power quality in distribution systems.

$$V_{drop(DOL)} = Z_{total} \times I_{start(Y-\Delta)} = 0{,}0796 \times 570{,}20 = 45{,}388 \text{ V}$$

Percentage flicker:

$$\%Flicker = \frac{V_{drop\ (DOL)}}{V_{rated}} \times 100\% = \frac{45{,}388}{419{,}10} \times 100\% = 11\%$$

The calculated flicker of 11% is significantly lower than the 32.48% observed with DOL starting. Although not entirely negligible, this level of flicker is typically more acceptable and highlights the Star-Delta method's effectiveness in mitigating voltage disturbances.

3.7 Discussion

This section presents the simulated flicker voltage profiles observed during the starting of a 250 kW three-phase induction motor using two different starting methods: Direct On Line (DOL) and Star-Delta. It compares the flicker voltage resulting from DOL starting with that produced by the Star-Delta method to highlight differences in their impact on system power quality. Flicker voltage refers to the time-varying deviation of the actual terminal voltage from its ideal sinusoidal waveform caused by the large inrush currents during motor starting. This phenomenon is a significant power quality concern in distribution networks, as severe voltage dips can lead to noticeable lamp flicker, malfunction of sensitive equipment, and diminished service quality for other customers connected at the same point of common coupling (PCC). The goal of this analysis is to evaluate the severity and waveform shape of voltage distortion caused by each starting technique, assess their relative impacts on system stability, and demonstrate the effectiveness of mitigation strategies such as the Star-Delta method in reducing voltage disturbances and maintaining acceptable power quality levels.

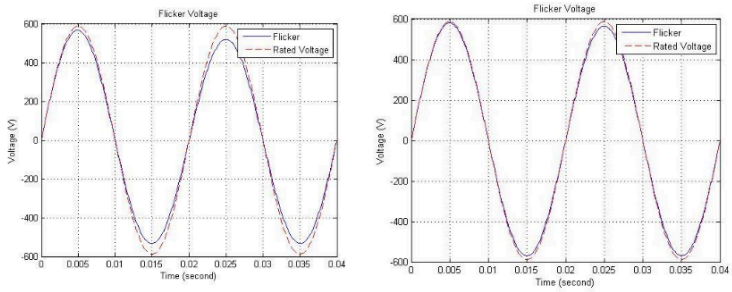

(a) (b)

Figure 1. Flicker voltage when starting with a difference: (a) DOL (b) Star-Delta

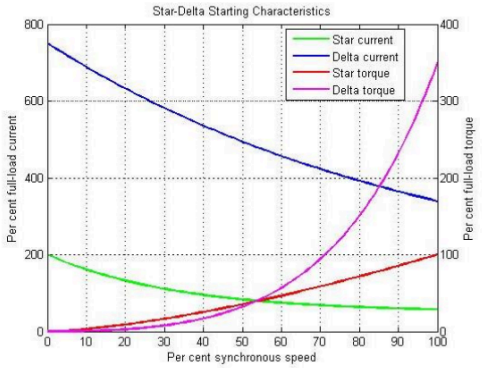

Figure 2. Comparison of current and torque characteristics for star and delta

Figure 1(a), which represents the DOL starting condition, it is clear that the flicker voltage waveform exhibits a pronounced deviation from the rated voltage sinusoid. The flicker voltage follows the same fundamental frequency but with noticeably larger amplitude modulation, reflecting a voltage drop of approximately 32.48 % as previously calculated. This severe voltage sag is a direct consequence of the high inrush current measured at approximately 2.88 times the motor's rated current drawn instantaneously when the motor is connected directly to the full supply voltage. The graph shows that the peak voltage during flicker is significantly reduced compared to the rated waveform, indicating that customers supplied by the same feeder could experience lighting flicker or voltage dips well beyond acceptable power quality limits defined in standards such as IEC 61000-3-3. In contrast, Figure 1(b) demonstrates the Star-Delta starting scenario, where the flicker voltage shows a visibly smaller deviation from the rated sinusoid. The voltage drop under this condition is reduced to about 11 %, consistent with the calculated starting current of approximately 0.96 times the rated current. The reduced inrush current during the initial star connection phase limits the magnitude of the voltage dip, producing a waveform that more closely matches the ideal sinusoid with only mild amplitude distortion. This difference illustrates the effectiveness of the Star-Delta method in mitigating voltage flicker, making it a preferred technique for starting large motors in distribution systems where voltage stability is a concern.

It is also noteworthy that while Star-Delta starting does not entirely eliminate flicker, the reduction in its severity makes it far more acceptable for most industrial and utility standards. This improvement not only enhances power quality for other customers but also reduces electrical and mechanical stresses on the motor itself, contributing to longer equipment lifespan and reduced maintenance costs. Furthermore, by comparing the two subplots, it becomes evident that adopting appropriate starting methods is a practical and economically viable strategy for utilities and facility managers seeking to minimize adverse power quality impacts without costly infrastructure upgrades. Figure 1 underscores the importance of starting method selection in large motor applications. By presenting a clear visual comparison between DOL and Star-Delta approaches, it highlights that technical planning and careful design choices can substantially improve network reliability, reduce customer complaints, and support broader objectives for sustainable and high-quality power distribution.

Figure 2 shows the comparison of current and torque behavior in star-delta starting methods for three-phase induction motors. It can be seen that in the star starting mode, the starting current (Star current) is much lower and drops steeply as synchronous speed increases, staying around 200% of full-load current at low speeds. This lower inrush current makes the star connection suitable for reducing starting current surges. In contrast, the delta starting mode (Delta current) has a much higher initial current, exceeding 700% of full-load current at zero speed, although it also decreases with speed. Regarding torque, the curve indicates that star mode torque (Star torque) is relatively low at the start and increases slowly, only approaching 100% of full-load torque near synchronous speed. Meanwhile, delta mode torque (Delta torque) is significantly higher, rising steeply to over 300% near full speed. This comparison explains why the star-delta method is used: it reduces starting current in the star connection phase and then switches to delta to provide the high torque required by the load. The graph clearly visualizes the trade-off between current and torque in both connection modes, highlighting the effectiveness of star-delta starting for controlling motor performance during startup.

4. CONCLUSION

Based on the analysis of flicker voltage profiles during the starting of a 250 kW three-phase induction motor using both Direct On Line (DOL) and Star-Delta methods, it can be concluded that the Star-Delta method is more effective in reducing voltage disturbances in the distribution system. The flicker voltage generated by the DOL method shows greater and more significant deviations from the ideal sinusoidal waveform due to the high inrush current, which can lead to power quality issues such as noticeable light flickering, malfunction of sensitive equipment, and reduced comfort for other consumers connected to the same point of common coupling. In contrast, the Star-Delta method produces a smoother flicker profile, closer to the nominal voltage, indicating a significant reduction in starting current and mitigation of voltage drop effects. Therefore, the application of the Star-Delta method is a practical solution for enhancing the stability of the power distribution system and maintaining service quality, especially in high-power motor applications that have a substantial impact on overall electrical system performance.

REFERENCES

[1] Widagdo, R. S., Asfani, D. A., & Negara, I. M. Y. (2021, October). Detection of Air Gap Eccentricity on Three-Phase Induction Motor Using 3-Axis Digital ELF Gaussmeter. In *2021 3rd International Conference on High Voltage Engineering and Power Systems (ICHVEPS)* (pp. 1-6). IEEE.

[2] Widagdo, R. S., Hartayu, R., & Hariadi, B. (2023). Discrete wavelet transform applied to 3-phase induction motor for air gap eccentricity fault diagnosis. *JEEMECS (Journal of Electrical Engineering, Mechatronic and Computer Science)*, *6*(2), 111-121.

[3] Widagdo, R. S., Hermawati, F. A., & Hariadi, B. (2024). Unbalanced Voltage Detection with Measurement Current Signature Analysis (MCSA) in 3-Phase Induction Motor Using Fast Fourier Transform (FFT). *Jurnal Teknologi Elektro*, *15*(02), 95-101.

[4] Widagdo, R. S., Andriawan, A. H., & Prenata, G. D. (2024). Impact of Ball Bearing Damage Variations on the Efficiency of Squirrel Cage 3-Phase Induction Motors. *RELE (Rekayasa Elektrikal dan Energi): Jurnal Teknik Elektro*, *7*(1), 218-225.

[5] Tampubolon, A. F., & Yana, S. (2013). *Analisis Kedip Tegangan Akibat Pengasutan Motor Induksi* (Doctoral dissertation, Universitas Sumatera Utara).

[6] Permana, A., Yuningtyastuti, Y., & Sukmadi, T. (2016). Analisis Pengaruh Metode Pengasutan Motor Induksi 3 Fasa Terhadap Kedip Tegangan yang Terjadi Pada Jaringan Kelistrikan PLTGU Blok I PT. Indonesia Power Up Semarang Menggunakan Simulasi Software ETAP 12.6. 0. *Transient: Jurnal Ilmiah Teknik Elektro*, *5*(2), 134-141.

[7] Altaira, M., Agela, G., & Issa, A. (2024, May). An Investigation into the Impact of Symmetrical Voltage Sag on the Performance of Three Phase Induction Motors-Based Simulation. In *2024 IEEE 4th International Maghreb Meeting of the Conference on Sciences and Techniques of Automatic Control and Computer Engineering (MI-STA)* (pp. 279-284). IEEE.

[8] Nema, B., & Tomar, S. (2024). A comprehensive review of induction motors: Principles, control techniques, and applications. *Research Journal of Engineering Technology and Medical Sciences*, *7*(1).

[9] Negi, G. S., Gupta, M. K., Saxena, N. K., & Mohan, H. (2024). Squirrel cage induction generator based micro grid voltage assessment with STATCOM using different metaheuristic approaches. *e-Prime-Advances in Electrical Engineering, Electronics and Energy*, *9*, 100736.

[10] Ghaseminezhad, M., Doroudi, A., Hosseinian, S. H., & Jalilian, A. (2021). High torque and excessive vibration on the induction motors under special voltage fluctuation conditions. *COMPEL-The international journal for computation and mathematics in electrical and electronic engineering*, *40*(4), 822-836.

[11] Ganesan, S., David, P. W., Balachandran, P. K., & Samithas, D. (2021). Intelligent starting current-based fault identification of an induction motor operating under various power quality issues. *Energies*, *14*(2), 304.

[12] Kucuk, S., & Ajder, A. (2022). Analytical voltage drop calculations during direct on line motor starting: Solutions for industrial plants. *Ain Shams Engineering Journal*, *13*(4), 101671.

[13] Jackson, O. I., Okpo, E. E., & Umoette, A. T. (2024). Comparative Analysis of Direct and Soft Starting Method for Induction Motor on Difference Load Levels. *Journal of Engineering Research and Reports*, *26*(10), 308-322.

[14] Pradana, M. R. R., Rahmawati, Y., & Putranto, H. (2021, October). Simulation of Using Dynamic Voltage Restorer Circuit For Analysis of Swell Voltage Repair in Three Phasse Induction Motor. In *2021 7th International Conference on Electrical, Electronics and Information Engineering (ICEEIE)* (pp. 96-99). IEEE.

[15] Al-Refai, S. M. (2023, May). Starting Analysis of Three-Phase Squirrel Cage Induction Motors. Case Study: Oil Production Field in Libya. In *2023 IEEE 3rd International Maghreb Meeting of the Conference on Sciences and Techniques of Automatic Control and Computer Engineering (MI-STA)* (pp. 117-123). IEEE.

Manuscript_BEES_Bima Gilang Pratama.pdf

ORIGINALITY REPORT

13%	9%	7%	7%
SIMILARITY INDEX	INTERNET SOURCES	PUBLICATIONS	STUDENT PAPERS

PRIMARY SOURCES

1	Submitted to UM Surabaya Student Paper	3%
2	ejurnal.seminar-id.com Internet Source	2%
3	www.scribd.com Internet Source	1%
4	studyelectrical.com Internet Source	1%
5	"IEEE MI-STA2023 Conference Proceeding", 2023 IEEE 3rd International Maghreb Meeting of the Conference on Sciences and Techniques of Automatic Control and Computer Engineering (MI-STA), 2023 Publication	1%
6	jist.publikasiindonesia.id Internet Source	1%
7	jurnal.unmer.ac.id Internet Source	1%
8	Submitted to School of Business & Computer Science Limited Student Paper	1%
9	Theoklitos S. Karakatsanis. "Optimization and Performance Evaluation of PM Motor and Induction Motor for Marine Propulsion Systems", Applied System Innovation, 2025 Publication	1%
10	Submitted to South Cheshire Student Paper	<1%

11	Submitted to Graphic Era University Student Paper	<1%
12	Submitted to Loughborough College Student Paper	<1%
13	Wang, Xiaoyu, Jing Yong, Wilsun Xu, and Walmir Freitas. "Practical Power Quality Charts for Motor Starting Assessment", IEEE Transactions on Power Delivery, 2011. Publication	<1%
14	Submitted to Blackpool and The Fylde College, Lancashire Student Paper	<1%
15	Submitted to Coleg Gwent Student Paper	<1%
16	Submitted to Fiji National University Student Paper	<1%
17	Khanh, Bach Q., J. Lian, B. Ramachandran, S. Srivastava, and D. Cartes. "Mitigating voltage sags due to DOL starting of three phase asynchronous motors using dynamic voltage restorer (DVR)", PES T&D 2012, 2012. Publication	<1%
18	journal2.unusa.ac.id Internet Source	<1%
19	Ermawati, Fadhli Palaha, Yolnasdi, Engla Harda Arya, Machdalena, Eki Yusrinal. "Analysis of Starting Current and Electrical Energy in Three Phase Induction Motor As A Chemical Processing System in PT Riau Andalan Pulp & Paper", 2022 9th International Conference on Electrical Engineering, Computer Science and Informatics (EECSI), 2022 Publication	<1%

20	M. Rajendra Rizky Pradana, Yuni Rahmawati, Hari Putranto. "Simulation of Using Dynamic Voltage Restorer Circuit For Analysis of Swell Voltage Repair in Three Phasse Induction Motor", 2021 7th International Conference on Electrical, Electronics and Information Engineering (ICEEIE), 2021 Publication	<1%
21	Manish K. Singh, Laetitia Cavellini, Maria Angeles Morcillo-Parra, Christina Kunz et al. "A constricted mitochondrial morphology formed during respiration", Nature Communications, 2025 Publication	<1%
22	Morteza Ghaseminezhad, Aref Doroudi, Seyed Hossein Hosseinian, Alireza Jalilian. "High torque and excessive vibration on the induction motors under special voltage fluctuation conditions", COMPEL - The international journal for computation and mathematics in electrical and electronic engineering, 2021 Publication	<1%
23	unsworks.unsw.edu.au Internet Source	<1%
24	www.researchgate.net Internet Source	<1%

Exclude quotes	On	Exclude matches	Off
Exclude bibliography	On		